

¹Physics Department,
Laser and Optics Center,
Shiraz University, Shiraz
71454, Iran,

²Physics Department,
Science and Research
Branch, Islamic Azad
University, Fars, Iran,

³Biostatistics Depart-
ment, Shiraz University
of Medical Science, Shi-
raz, Iran.

Photothermal Effect of Laser on Mole Removal: Analytical Model and Laser Suitability

Nadgaran H.¹, Mahmoodi M.^{2*}, Mahmoodi M.³

Since 1960, laser has been very attractive to researchers of medical sciences [1, 2]. Lasers are commonly used in dentistry, cancer therapy, dermatology, ophthalmology, and gastrointestinal diseases [3, 4].

Laser characteristics made it a unique surgical blade with least side effects and minimum bleeding. Certain physical parameters play important roles in using lasers. These parameters include tissue irradiation time, laser wavelength, and laser energy density; lasers with power densities less than 0.1 W/cm² can cause photochemical reaction on the tissue. However, thermal effects [5, 6] can occur by using lasers with power densities lesser than 10⁵ W/cm². To ablate a piece of tissue, the laser power densities must exceed 10⁹ W/cm² [7]. Very high power laser can take the tissue to a near ionization state and even can dissociate the tissue in atomic and molecular levels to form dense plasmas.

Herein, we describe the photothermal effect of laser on moles. For this reason, certain optical properties of the mole such as its absorption coefficient for different laser wave lengths are also important.

It is shown [8] that tissues experiencing a total temperature rise of 5 °C are usually not damaged. On the other hand measurement of such tiny damages is a challenging task. However, temperature rises above 42 °C can irreversibly harm the tissues by denaturing proteins [9, 10].

This study mostly deals with various laser systems that do not produce severe thermal effects on tissues and that are very less harmful. To do so, the profile of temperature rising of a mole when exposed to various lasers was studied. First, the thermal equation for nearly spherical moles was solved analytically when the mole absorption coefficient was explicitly taken into account. By reporting the numeric values of the temperature rise, we could then select the most appropriate laser system with the least harm to the tissues, for mole removal.

Assuming that the mole has a spherical shape (Fig. 1), the following equations govern T_1 and T_2 :

$$0 \leq \theta \leq \theta_0 \Rightarrow K \nabla^2 T_1 = Q_0 e^{-\alpha a} \quad \text{and}$$

$$\theta_0 \leq \theta \leq \pi \Rightarrow K \nabla^2 T_2 = Q_0 e^{-2\alpha a} \quad (1)$$

where θ_0 denotes the polar angle in spherical coordinates, α shows the

*Corresponding author:
Maryam Mahmoodi,
Tel: +917-125-2778
E-mail: maryam19258@gmail.com,

mole absorption coefficient, K is the thermal conductivity of the mole and a is the radius of the mole.

As the maximum temperature rise occurs on the mole surface, the boundary conditions would be:

$$\theta = \theta_0 \Rightarrow T_1 = T_2 = T_0 \quad \text{and}$$

$$r = a \Rightarrow \frac{\partial T_1}{\partial r} = 0 \quad (2)$$

The latter boundary condition was used because two distinct regions were defined for the

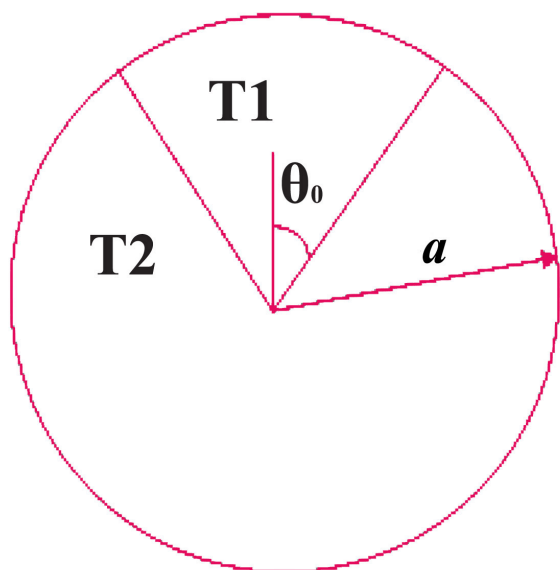


Figure 1: Spherical model for a mole

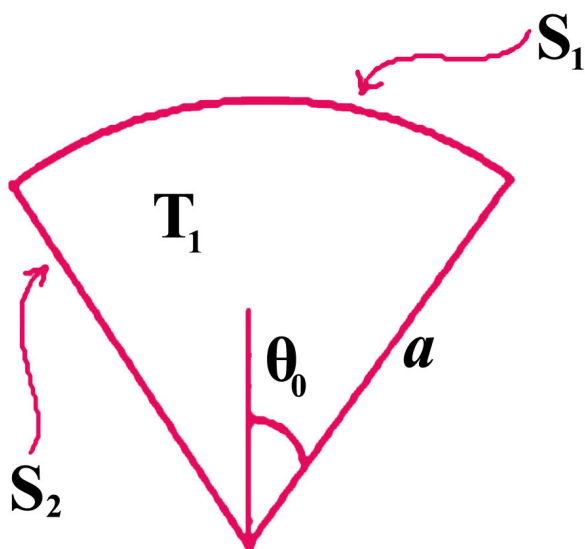


Figure 2: The first region and boundary surfaces

Table 1: Laser systems used in mole removal operations

Laser type	λ (nm)	α (cm ⁻¹)
Nd:Yag	1064	0.385
Er:Yag	2940	2.127
Co ₂	10600	2.3
Alexandrite	750	8.1

mole (Fig. 1), and along the boundary of this region the temperature rise had to be kept the same.

To solve the thermal equation (Eq. 1), considering the symmetry of the problem in spherical coordinates, we used the Green function formulation of:

$$G(r, \theta) = 4\pi \sum_l \sum_m \frac{Y_{lm}^*(\theta', \phi') Y_{lm}(\theta, \phi)}{2l+1} \times r_l^l \left(\frac{1}{r_l^{l+1}} - \frac{r_l^l}{a^{2l+1}} \right) \quad (3)$$

Upon using this method, one can set:

$$T_1(r, \theta) = \frac{1}{4\pi K} \int Q_0 e^{-\alpha a} G(r', \theta') dV + \frac{1}{4\pi} \oint_{s_1} G \frac{\partial T_1}{\partial n'} da' - \frac{1}{4\pi} \oint_{s_2} T_1(r', \theta') \frac{\partial G}{\partial n'} da' \quad (4)$$

The right side of Eq. 4 shows two surface integrals on s_1 and s_2 (Fig. 2).

After the same mathematical manipulation, we finally end up with T_1 as:

$$T_1(r, \theta) = \frac{Q_0 e^{-\alpha a}}{2K} \sum_l \left[\frac{1}{2l+1} (P_{l+1}(\cos \theta_0) - P_{l-1}(\cos \theta_0)) \right] \times \left[\left(\frac{r^{l+3}}{l+3} \right) \left(\frac{1}{r^{l+1}} - \frac{r^l}{a^{2l+1}} \right) + \frac{(2l+1)a^{2-1}}{(2-l)(3+l)} r^l - \frac{r^{2-l}}{(2-l)} + \frac{r^{l+3}}{a^{2l+1}(l+3)} \right] \times P_l(\cos \theta) + \frac{T_0 \sin \theta_0}{2} \sum_l \left(\frac{r^{l+2}}{l+2} \right) \left(\frac{1}{r^{l+1}} - \frac{r^l}{a^{2l+1}} \right) P_l(\cos \theta) + \frac{T_0 \sin \theta_0}{2} \sum_l \left[\frac{(2l+1)}{(1-l)(2+l)} r^l a^{1-l} - \frac{r^{1-l}}{(1-l)} + \frac{r^{l+2}}{a^{2l+1}(l+2)} \right] P_l(\cos \theta) \times (-\sin \theta_0) \left[\frac{(l+1)(\cos \theta_0) P_l(\cos \theta_0)}{\sin^2 \theta_0} - \frac{l+1}{\sin^2 \theta_0} P_{l+1}(\cos \theta_0) \right]$$

To find T_2 , one should note that the boundary condition employed for the calculation of T_1 is no longer valid. But as T_2 must bear a maximum value at $\theta = \theta_0$ and a minimum at $\theta = \pi$, we are facing two extremum values in T_2 region.

With this formalism, T_2 would be:

$$T_2(r, \theta) = \frac{Q_0 e^{-2\alpha a}}{2K} \sum_l \left\{ \left[\left(\frac{r^{l+3}}{l+3} \right) \left(\frac{1}{r^{l+1}} \frac{r^l}{a^{2l+1}} \right) + \frac{(l-1)a^{2-l}}{2-l} r^l \right] \right. \\ \times [P_{l-1}(\cos \theta_0) - P_{l+1}(\cos \theta_0) \times P_l(\cos \theta)] \\ - \frac{T_0}{2} \sum_l \frac{(2l+1)a^{l-l}}{(2+l)(1-l)} r^l P_l(\cos \theta) \times (l+1) \\ \times [(\cos \theta_0) P_l(\cos \theta_0) - P_{l+1}(\cos \theta_0)] \\ \left. - \sum_l P_l(\cos \theta) \times \left[\left(\frac{r^{l+2}}{l+2} \right) \left(\frac{1}{r^{l+1}} \frac{r^l}{a^{2l+1}} \right) + \frac{(2l+1)}{(1-l)(2+l)} r^l a^{1-l} \right] \right. \\ \left. \times \left[\frac{12}{15} \cos \theta_0 - \frac{32}{105} + \frac{1}{3} (\cos \theta_0 - 1) \times [P_{l+1}(\cos \theta_0) - P_{l-1}(\cos \theta_0)] \right] \right\}$$

Table 1 shows the laser characteristics of four systems which are frequently used in mole removal operations along with mole radius, a , θ_0 , and K values.

- $a = 1.4 \text{ mm}$
- $Q_0 = 50 \text{ J}$
- $\theta_0 = 6^\circ \text{C}$
- $K = 1.6$

Figure 3 shows T_1 vs. r , which is the distance from top to the center of the mole taken as the coordination origin for different lasers. The figure shows the maximum temperature rise at the surface of the top down to the center of the mole.

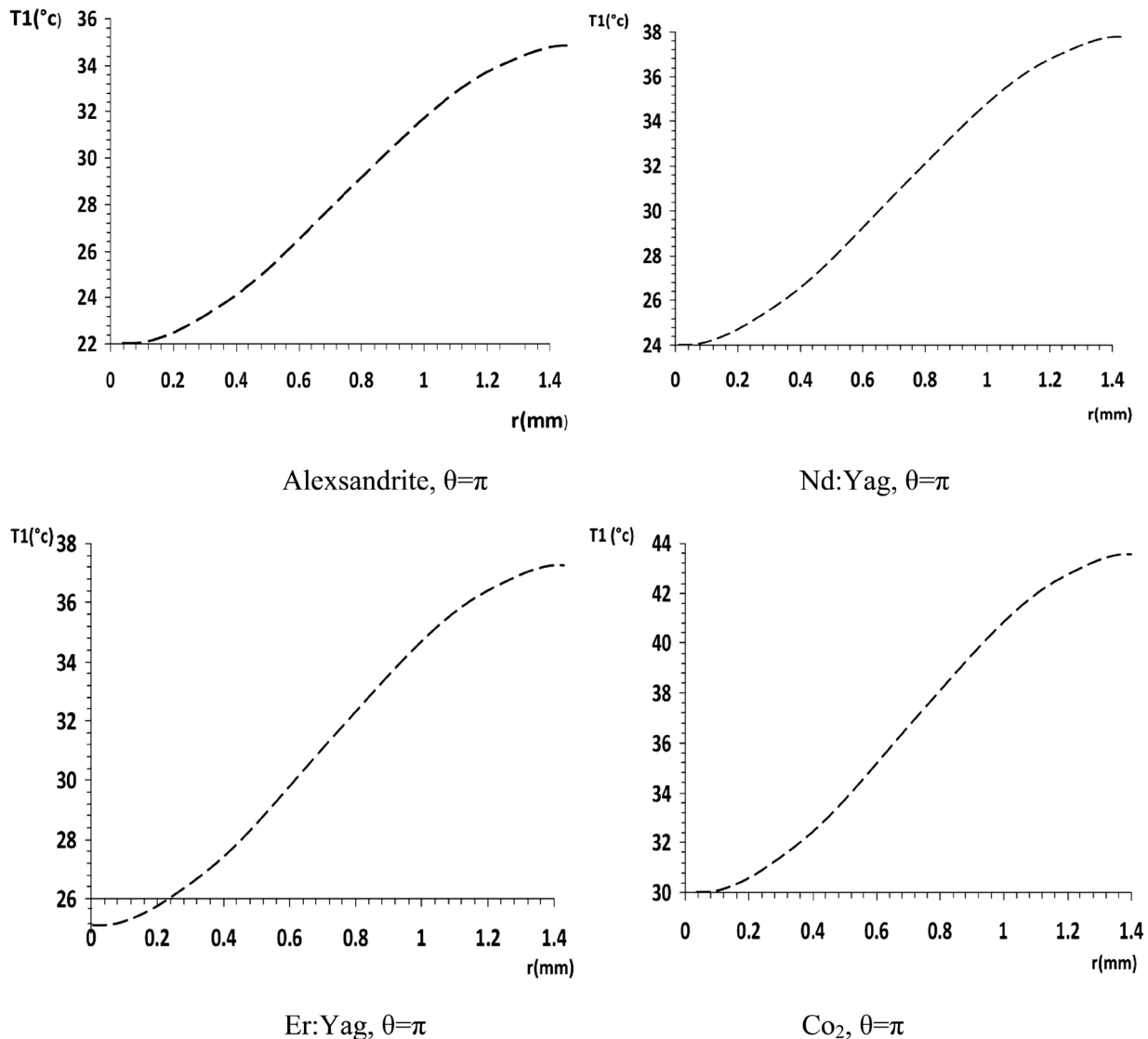


Figure 3: The distance from top to the center the mole taken as the coordination origin, for various lasers

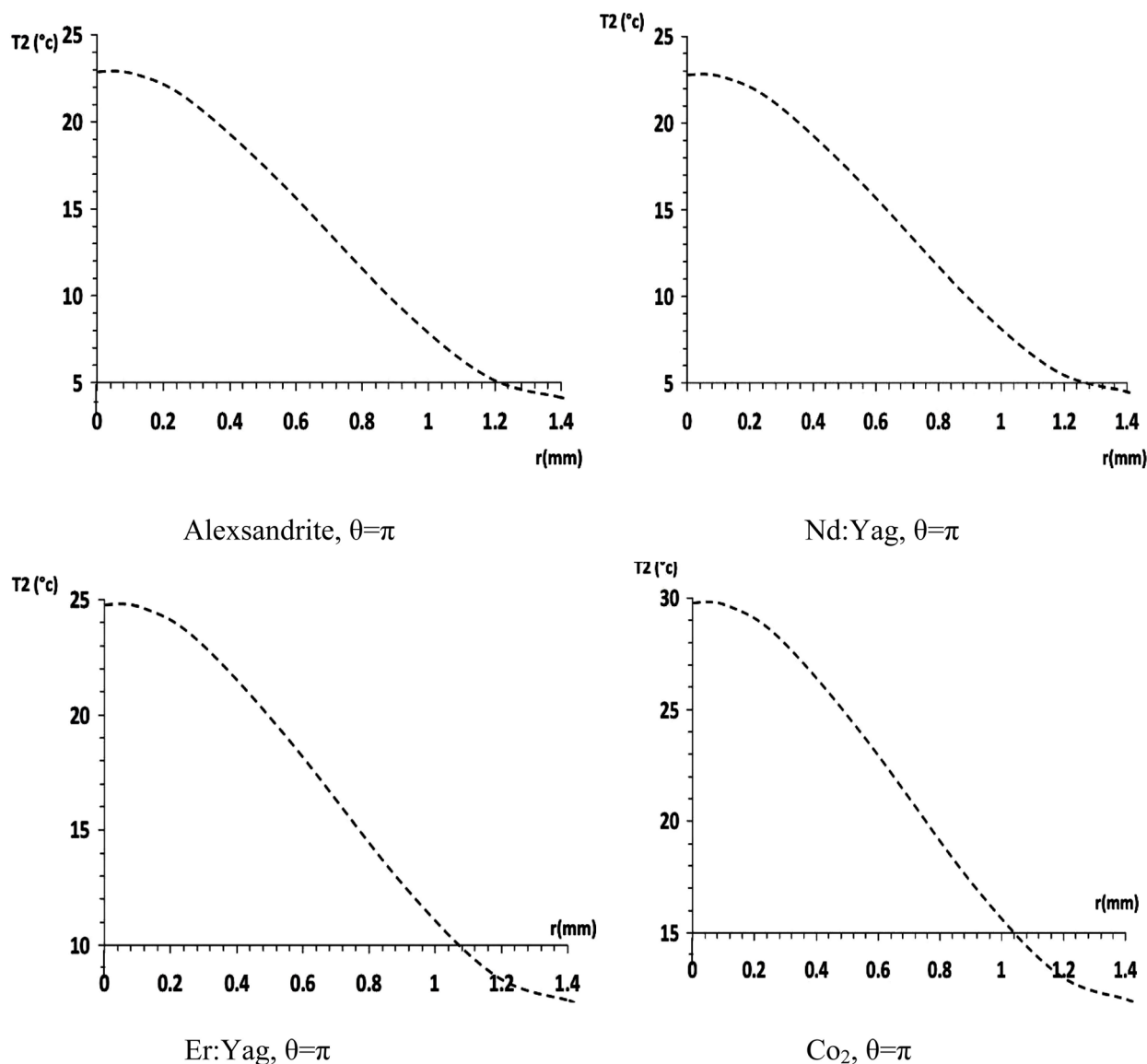


Figure 4: The reduction in temperature rise when r increases, also for the four studied lasers

Figure 4 depicts T_2 vs. r . This graph shows the reduction in temperature rise when r increases.

As was clearly shown, it is evident that among the four laser systems studied, Alexandrite and Nd:Yag lasers produced the minimum temperature rise at the mole contact with the skin, and thus are more suitable than Er:Yag and CO₂ lasers. This underlines the fact that in selecting an appropriate laser for mole removal, both the absorption rate of the mole and the temperature rise distribution profile should be considered.

References

1. Maiman T. Stimulated optical radiation in ruby. *Nature* 1960;**187**:493-4.
2. Huang H, Guo Z. Ultrashort pulsed laser ablation and stripping of freeze-dried dermis. *Lasers in medical science* 2010; **25**:517-24.
3. Guo Z, Wan SK, August DA, *et al.* Optical imaging of breast tumor through temporal log-slope difference mappings. *Comput Biol Med* 2006; **36**:209-23
4. Moshonov J, Stabholz A, Leopold Y, Rosenberg I. [Lasers in dentistry- Part B-Interaction with biological tissues and effect On the Soft tissues of the oral Cavity the hard tissues of the dental pulp.] *Refuat Happen Vehashinayim* 2001;**18**:21-

- 8.
5. Jiao J, Guo Z. Thermal interaction of short-pulsed laser focused beams with skin tissues. *Physics in medicine and biology* 2009;**54**:4225.
6. Cummins L, Nauenberg M. Thermal effects of laser radiation in biological tissue. *Biophysical journal* 1983;**42**:99-102.
7. Chen B, Thomsen SL, Thomas RJ, Welch AJ. Modeling thermal damage in skin from 2000-nm laser irradiation. *J Biomed Opt* 2006;**11**:1-15
8. Markolf H. Niemz. *Laser-Tissue Interactions: fundamentals and applications*. Third enlarge edition, Springer-Verlag **2007**.
9. Lowe NJ, Lask G, Griffin ME, *et al*. Skin resurfacing with the Ultrapulse carbon dioxide laser. Observations on 100 patients. *Dermatol Surg* 1995;**21**:1009-25.
10. Sheehan-Dare R.A, Coterill J.A. Lasers in Dermatology. *Br J Dermatol* 1993;**129**:1-8.